Diffraction theory of general nondiffracting beams generated with finite-aperture systems

E. Carcolé *

Laboratori de Física Teòrica, Department d'Optica, Apartado de Correos 326, 43500 Tortosa, Spain

Abstract

In this paper, we solve the Fresnel diffraction integral corresponding to the propagation of a general nondiffracting beam generated from an arbitrary finite-aperture system. The solution contains the original infinite-extent nondiffracting beam times a modulating function which does not depend on the nondiffracting beam being generated. The modulating function corresponds to an average taken on a ring of the diffraction pattern of the aperture centered at the point where the performance has to be evaluated. The solution also contains additive functions that become important when the ring has a section lying outside the geometrical projection of the aperture. As an example, we show that the performance of a J_0 beam diffracted by a circular aperture may be intuitively understood from the characteristics of the diffraction pattern of a circular aperture.

1. Introduction

The scalar theory of nondiffracting beams (NBs) was first introduced by Durnin [1]. The first experimental investigation of these beams showed that the theory was in agreement with experimental results [2]. The scalar-wave equation for free space has infinite diffraction-free solutions. The spatial spectrum of those solutions is confined to a single ring in the spatial-frequency domain [3]; amplitudes and phases on the ring can be arbitrary. Some solutions can be described by known functions; important examples are the Bessel beams [3], the Mathieu beams [4,5] and the parabolic beams [6]. Other solutions can be written using modified Bessel functions [7], Hankel functions [8], and Weber functions [9]. The freedom of the amplitude and phase in the spatial spectrum of the solutions can be applied to

---
* Tel./fax: +34 936 661710.
E-mail address: ecarcole@yahoo.com.

design NBs [10]. Also, the superposition of NBs with different frequencies (nondiffracting X and Y waves) has been considered in order to obtain diffraction-free and dispersion-free pulsed beams [11].

There are a number of methods by which to generate optical NBs [12]. With the axicon [13,14], with lenses with spherical aberration [12] and with the Fabry–Perot interferometer [15] zero-order Bessel beams may be generated with high diffraction efficiency. Axicon-type computer-generated holograms have been used to generate the zero-order and higher-order Bessel beams [16,17]. This type of hologram may be generated too with programmable spatial light modulators [18,19] allowing the real time variation of the size and the deflection angle of the beam. Long-range Bessel beams can be generated with optical systems with spherical aberration [20]; propagation distances over 500 m may be obtained [21]. Zero order [22] and higher-order [23] Mathieu beams may be generated too using computer generated phase holograms. Acoustic NBs have been generated with two-dimensional ultrasonic transducers [24].

The properties [12,25] of NBs are useful for several applications; some examples: axial and angular alignment [26], large size measurement [27], scanning optical systems [14], optical interconnections [28], range-finding by triangulation [29], optical tweezers [30] and optical microlithography [31].

It is not possible to generate a NB exactly because such a beam has infinite extent. Analytical expressions for the transverse and axial intensity distributions associated with J_0 Bessel beams [32,33] and J_0 Bessel–Gauss [33] beams propagating from a circular aperture have been obtained in the Fresnel diffraction approximation for both the far field and the near field in order to describe diffraction effects on those beams; those expressions contain integrals or infinite series which have to be evaluated numerically in order to establish some general propagation features of those beams. Phase stationary principle has been used to demonstrate that axicon-type [16,17] holograms generates Bessel beams. It also allows to describe certain properties of generalized axicons [34], but the use of this mathematical approximation does not permit an accurate analysis of diffraction effects in a general case. Still geometrical optics is the only tool used in the derivation of the expressions to calculate the maximum distance of propagation [1] and the distance at which self-regeneration properties become evident [25,30].

The aim of this paper is to develop an analysis based on the Fresnel diffraction theory [35] in order to calculate diffraction effects on general NBs generated from an arbitrary system with finite aperture. An analytical expression with a simple physical meaning that allows taking into account all diffraction effects as a function of the Fresnel diffraction pattern of the aperture will be developed. Then, in Section 2, we will make some definitions and we will introduce the basic facts of NBs which are important for our development. The analysis will be developed in Section 3: we will solve the Fresnel diffraction integral corresponding to the propagation of a general nondiffracting beam generated from an arbitrary finite-aperture system; the solution we will find out contains the original infinite-extent nondiffracting beam times a modulating function which does not depend on the nondiffracting beam being generated. The modulating function will corresponds to an average taken on a ring of the diffraction pattern of the aperture centered at the point where the performance has to be evaluated. This ring will have a radius proportional to the wavelength and the distance from the aperture and will be inversely proportional to a scale factor of the nondiffracting beam. The solution will also contain additive functions that become important when the ring has a section lying outside the geometrical projection of the aperture. In order to show how to use our theory to describe an arbitrary beam, a particular case will be discussed: the propagation of a J_0 beam generated from a circular aperture. Then, in Section 4 some important characteristics of the diffraction pattern of a circular aperture are derived. In Sections 5 and 6 the behavior of a J_0 beam is analyzed and described from the characteristics of the diffraction pattern of the circular aperture. In Section 7 illumination with a diverging spherical wave is considered in order to obtain long range NBs.

2. Theoretical background. Notation

2.1. General expression for NBs

A general NB propagating in the z-axis direction may be written as

$$b(r', \theta, z) = k_r \exp(ik_z z) \int_0^{2\pi} A(\varphi)$$
$$\times \exp[ik_r r' \cos(\theta - \varphi)] d\varphi, \qquad (1)$$

where $k_z^2 + k_r^2 = k^2$, k is the wave number and $A(\varphi)$ is an arbitrary complex function. The spatial spectrum can be obtained performing the two-dimensional Fourier Transform (FT) of $b(r', \theta, z)$:

$$B(\eta, \varphi, z) = A(\varphi) \exp(ik_z z) \delta\left(\eta - \frac{1}{r_0}\right), \qquad (2)$$

where $r_0 = 2\pi/k_r$. This equation means that the spatial spectrum of any NB is composed of plane-waves whose wave vectors describe a circumference. Bessel beams of n-order are obtained by using [3]:

$$A(\varphi) = \frac{r_0 i^{-n}}{(2\pi)^2} \exp(in\varphi) \qquad (3)$$

in Eq. (1). Every type of NB has a different definition for the function $A(\varphi)$.

A truly NB is unlimited in transverse extent. We will use the notation NB when the transverse extent is unlimited. We will use the notation Size-limited NB (SNB) when the transverse extent is limited and diffraction effects arise.

2.2. Fresnel number

For our development, we will have to consider the diffraction of the aperture of the SNB (for instance, the diffraction of a circular aperture) at the distance z from the aperture where the performance of the SNB should be evaluated. A convenient parameter that allows characterizing a diffraction pattern is the Fresnel number [36] N_F. For a circular aperture of radius R, illuminated with a monochromatic plane-wave of wavelength λ it is defined as:

$$N_F = \frac{R^2}{\lambda z}. \qquad (4)$$

For a square aperture, R is half the length of its side. Fresnel number coincides with the number of maxima in the transverse intensity distributions for the diffraction pattern of a circular or square aperture.

2.3. Calculating and representing Fresnel diffraction patterns

Let us suppose a setup that generates a SNB by illuminating a diffractive element (DE) with a monochromatic plane wave (later we consider the most general case). Let us define the Cartesian coordinates $\mathbf{r} = (x,y)$ in the plane $z = 0$. We define a function $t(\mathbf{r})$ corresponding to the transmittance of the DE. The diffraction pattern generated by the DE when it is illuminated with a monochromatic plane wave $A \exp(ikz)$, where A is the amplitude of the plane wave, may be calculated by using the Fresnel diffraction theory as follows [36]: $D(\mathbf{r}',z) = (A \exp(ikz)/i\lambda z)t(\mathbf{r}) * Z(\mathbf{r},z)$ where $Z(\mathbf{r},z) = \exp[i(k/2z)r^2]$ and $\mathbf{r}' = (x',y')$ are the Cartesian coordinates in the plane where the diffraction pattern is calculated; also the corresponding cylindrical coordinates (r',θ) will be used. The symbol $*$ stands for convolution. It is convenient to define a new function $s(\mathbf{r}',z)$:

$$s(\mathbf{r}', z) = \frac{\exp(ikz)}{i\lambda z} t(\mathbf{r}) * Z(\mathbf{r}, z). \qquad (5)$$

Evidently $s(\mathbf{r}',z) = D(\mathbf{r}',z)/A$. Working with the function $s(\mathbf{r}',z)$ has two advantages: (i) It has no units, this allows to avoid the "arbitrary units" expression in graphic representations of $|s(\mathbf{r}',z)|$ or $|s(\mathbf{r}',z)|^2$ used by many authors; (ii) It is a normalised function: $|s(\mathbf{r}',z)| = 1$ for $t(\mathbf{r}) = 1$ (which may correspond to the diffraction of an infinite-sized aperture). Then, we will use Eq. (5) for the calculation of Fresnel diffraction patterns.

Any experimental setup that generates an electromagnetic or acoustical SNB from a certain plane ($z = 0$) without the use of a DE may be analyzed as well with Eq. (5) by defining a "virtual transmittance function" with the following equality: $t(\mathbf{r}) = s(\mathbf{r},z = 0)$. This assures that our treatment may be used in a general case. A good example of this is the original experimental setup used by Durnin et al. [2], which is evidently

equivalent to having a DE with a transmittance function that may be written as a J_0 times a circular aperture.

In graphical representations of diffraction patterns we will represent the amplitude $|s(\mathbf{r}',z)|$ instead of the intensity. This will make it easier to visualize the diffraction effects in the points far from the optical axis. For the particular case of a Bessel function of arbitrary order, it is important to note that it is not square integrable because every ring contains about the same amount of energy, and from this point of view, they all have the same importance. Then, we believe that it is important, from a physical point of view, to clearly show the diffraction effects even for points far from the optical axis because those effects imply a important redistribution of energy in the beam.

Finally, we are going to use the expression "geometrical projection of the aperture" in its rigorous mathematical meaning. In several sections in this paper, we will consider a circular aperture of radius R, centered at the optical axis and containing a DE that generates the SNB. Then, the geometrical projection of this aperture at a distance z corresponds to another circle with the same radius R also centered at the optical axis.

2.4. Fourier transforms

The FT and the inverse FT (with a scale given by λz) of a certain function $h(\mathbf{r})$ are defined by the following equalities:

$$H(\mathbf{u}) = F_{\lambda z}[h(\mathbf{r})](\mathbf{u}) = \int \int \exp\left(-\frac{2\pi i}{\lambda z}\mathbf{r} \cdot \mathbf{u}\right)h(\mathbf{r})d\mathbf{r},$$

$$h(\mathbf{r}) = F_{\lambda z}^{-1}[H(\mathbf{u})](\mathbf{r})$$
$$= \frac{1}{(\lambda z)^2} \int \int \exp\left(+\frac{2\pi i}{\lambda z}\mathbf{r} \cdot \mathbf{u}\right)H(\mathbf{u})d\mathbf{u}.$$
(6)

3. Diffraction of general SNBs

In this section, we will solve the Fresnel diffraction integral corresponding to the propagation of a general nondiffracting beam generated from a finite-aperture system. We solve the integral in a way that allows writing the final solution as the product of the original infinite-extent nondiffracting beam times a modulating function which will be a function of the diffraction pattern of the aperture but will not depend on the nondiffracting beam being generated. The solution will also contain additive functions that will be easily written in terms of known functions for the particular case of a Bessel beam of arbitrary order. In order to get this result, we have to transform the diffraction integral in a way that may look quite artificial, but the final solution will be simple and meaningful and will provide physical insights on how the nondiffracting pattern is affected by the aperture.

We start by writing the transmittance function $t(\mathbf{r})$ of the DE as follows:

$$t(\mathbf{r}) = p(\mathbf{r})b(\mathbf{r}, 0),$$
(7)

where $b(\mathbf{r},0)$ is the complex amplitude corresponding to a general NB as defined in Eq. (1) for $z = 0$ and $p(\mathbf{r})$ is a generalized pupil function that may written as the product of four functions that takes into account several facts: (i) the aperture function that takes into account the finite size of the DE; (ii) a function describing any errors in the encoding process of the DE [37]; (iii) a function that takes into account any kind of apodization [38]; (iv) a function that takes into account the illumination of the DE by an arbitrary beam (in the case of an optical SNB); this function corresponds to the complex amplitude of the arbitrary beam in the plane $z = 0$ (DE's plane). The particular case of spherical wave illumination will not supposed to be included in the pupil function and it will be studied in Section 7 in order to increase the range of the SNB.

It is also possible to define $p(\mathbf{r})$ as follows: $p(\mathbf{r}) = s(\mathbf{r},0)/b(\mathbf{r},0)$. This definition may be the most convenient when the beam is generated without the use of a DE.

The Fresnel diffraction integral at a distance z from the DE may be written as a FT [39]:

$$s(\mathbf{r}',z) = \frac{\exp(ikz)}{i\lambda z}Z(\mathbf{r}',z)F_{\lambda z}[Z(\mathbf{r},z)t(\mathbf{r})](\mathbf{r}',z).$$
(8)

The calculation of the diffraction integral will be performed in several steps.

3.1. First step

First, we will write the diffraction field of a SNB as a convolution of the diffraction of a NB with the FT of the pupil function. The propagation of the NB is a known function, so a first simplification of the integral will be obtained. Using a basic property of FT [39] (the FT of the product of two functions may be written as the convolution of the FT of each function) and Eq. (7) we may transform Eq. (8):

$$s(\mathbf{r}',z) = \left(\frac{1}{\lambda z}\right)^2 Z(\mathbf{r}',z)\left[\left\{Z^{-1}(\mathbf{r}'',z)N(\mathbf{r}'',z)\right\}\right.$$
$$\left. *F_{\lambda z}[p(\mathbf{r})](\mathbf{r}'',z)\right], \tag{9}$$

where $\mathbf{r}'' = (x'',y'')$ are the Cartesian coordinates in the plane where the convolution is carried out and

$$N(\mathbf{r}'',z) = \frac{\exp(\mathrm{i}kz)}{\mathrm{i}\lambda z}Z(\mathbf{r}'',z)F_{\lambda f}[Z(\mathbf{r},z)b(\mathbf{r},0)](\mathbf{r}'',z), \tag{10}$$

$N(\mathbf{r}'',z)$ corresponds to the Fresnel diffraction of a general NB and can be written as a convolution integral: $N(\mathbf{r}'',\psi) = (\exp(\mathrm{i}kz)/\mathrm{i}\lambda z)b(\mathbf{r},0)*Z(\mathbf{r},z)$. This convolution integral can be solved analytically by performing the Fourier transform of $N(\mathbf{r}'',z)$ and using Eq. (2):

$$F[N(\mathbf{r}'',z)](\eta,\varphi) = \frac{\exp(\mathrm{i}kz)}{\mathrm{i}\lambda z}A(\varphi)\delta\left(\eta - \frac{1}{r_0}\right)\lambda z$$
$$\times \exp(-\mathrm{i}\pi\lambda z\eta^2)$$
$$= \frac{1}{\mathrm{i}}\exp(\mathrm{i}kz)\exp\left(-\mathrm{i}\pi\frac{\lambda z}{r_0^2}\right)B(\eta,\varphi,0). \tag{11}$$

Performing the inverse Fourier transform we obtain: $N(\mathbf{r}'',z) = \exp(\mathrm{i}kz - \mathrm{i}\pi\lambda z/r_0^2)b(\mathbf{r}'',0)$. The complex exponential function corresponds to a paraxial approximation of $\exp(\mathrm{i}k_z z)$. Then, for the sake of shortness and correctness we may write with no loss of accuracy $N(\mathbf{r}'',z) = b(\mathbf{r}'',z)$; using this in Eq. (9), we obtain:

$$s(\mathbf{r}',z) = \left(\frac{1}{\lambda z}\right)^2 Z(\mathbf{r}',z)\left[\left\{Z^{-1}(\mathbf{r}'',z)b(\mathbf{r}'',z)\right\}\right.$$
$$\left. *F_{\lambda z}[p(\mathbf{r})](\mathbf{r}'',z)\right]. \tag{12}$$

3.2. Second step

We wish now to write Eq. (12) as a convolution integral of $b(\mathbf{r}'',z)$ with another function. Note that this should allow an easy calculation of $s(\mathbf{r}',z)$ just by performing its FT, because the FT of $b(\mathbf{r}'',z)$ in Eq. (2) is written in terms of a delta function. Taking into account that convolution is a commutative operation and the following equality: $Z^{-1}(\mathbf{r}' - \mathbf{r}'',z) = Z^{-1}(\mathbf{r}'',z)Z^{-1}(\mathbf{r}',z)\exp(\mathrm{i}(2\pi/\lambda z)\mathbf{r}'\mathbf{r}'')$, we may rewrite Eq. (12) as:

$$s(\mathbf{r}',z) = \frac{1}{(\lambda z)^2}\int\int \exp\left(\mathrm{i}\frac{2\pi}{\lambda z}\mathbf{r}'\cdot\mathbf{r}''\right)Z^{-1}(\mathbf{r}'',z)$$
$$\times F_{\lambda z}[p(\mathbf{r})](\mathbf{r}'',z)b(\mathbf{r}' - \mathbf{r}'',z)\mathrm{d}\mathbf{r}''. \tag{13}$$

Let us notice here a key point for our analysis. Note that the coordinates $\mathbf{r}'$ are parameters in the integral. This fact will allow us to perform a non-conventional analysis of this kind of integral. Let us define a 5-dimensional function $s'(\mathbf{r}',\mathbf{w},z)$ (where $\mathbf{w} = (u,v)$ and u and v are new Cartesian coordinates) that will be equivalent to $s(\mathbf{r}',z)$ for $\mathbf{w} = \mathbf{r}'$:

$$s'(\mathbf{r}',\mathbf{w},z) = \frac{1}{(\lambda z)^2}\int\int \exp\left(\mathrm{i}\frac{2\pi}{\lambda z}\mathbf{r}''\cdot\mathbf{w}\right)Z^{-1}(\mathbf{r}'',z)$$
$$\times F_{\lambda z}[p(\mathbf{r})](\mathbf{r}'',z)b(\mathbf{r}' - \mathbf{r}'',z)\mathrm{d}\mathbf{r}''. \tag{14}$$

This allows us to rewrite this integral as a convenient convolution integral (integrating the coordinate $\mathbf{r}''$):

$$s'(\mathbf{r}',\mathbf{w},z) = \frac{1}{(\lambda z)^2}g(\mathbf{r}'',\mathbf{w},z)*b(\mathbf{r}'',z), \tag{15}$$

where

$$g(\mathbf{r}'',\mathbf{w},z) = \exp\left(\mathrm{i}\frac{2\pi}{\lambda z}\mathbf{w}\cdot\mathbf{r}''\right)Z^{-1}(\mathbf{r}'')F_{\lambda z}[p(\mathbf{r})](\mathbf{r}''). \tag{16}$$

Now, we will perform the FT of $s'(\mathbf{r}',\mathbf{w},z)$ *integrating the coordinates* $\mathbf{r}'$. The resulting function will not be the spatial spectrum of the diffracted field, but a simple function (that may be denoted as a point-dependent pseudo-spectrum) that will allow to easily perform a meaningful analysis. After this analysis an inverse FT will be performed and then we will use $\mathbf{w} = \mathbf{r}'$. If we wish to calculate

the FT of $s'(\mathbf{r}',\mathbf{w},z)$ we need to calculate the FT of the functions $b(\mathbf{r}'',z)$ and $g(\mathbf{r}'',\mathbf{w},z)$. This will be calculated in the third step.

3.3. Third step

Let us write the FT of the function $g(\mathbf{r}'',\mathbf{w},z)$:

$$G(\mathbf{v},\mathbf{w},z) = F_{\lambda z}\left(\exp\left(\mathrm{i}\frac{2\pi}{\lambda z}\mathbf{w}\cdot\mathbf{r}''\right)Z^{-1}(\mathbf{r}'',z)\right.$$
$$\left.\times F_{\lambda z}[p(\mathbf{r})](\mathbf{r}'',z)\right)(\mathbf{v},z), \qquad (17)$$

the Cartesian coordinates in the Fourier plane will be denoted $\mathbf{v} = (v_x,v_y)$ and (σ,α) the corresponding cylindrical coordinates. This expression may be rewritten as the convolution of three FT's with Cartesian coordinates $\mathbf{v}' = (v'_x, v'_y)$. Using the associative property of the convolution operation we may write Eq. (17) as follows:

$$G(\mathbf{v},\mathbf{w},z) = \mathrm{i}(\lambda z)^4 \exp(-\mathrm{i}kz)\left[\frac{\exp(\mathrm{i}kz)}{\mathrm{i}\lambda z}p(-\mathbf{v}') * Z(\mathbf{v}',z)\right]$$
$$* \delta(\mathbf{v}' - \mathbf{w}). \qquad (18)$$

The second key point in our analysis is that the term between square brackets is the Fresnel diffraction pattern of $p(-\mathbf{v}')$ at a distance z. The convolution of the delta function will shift this diffraction pattern, and then, after the convolution it may be denoted as $P(-(\mathbf{v}-\mathbf{w}),z)$. Eq. (18) becomes:

$$G(\mathbf{v},\mathbf{w},z) = \mathrm{i}(\lambda z)^4 \exp(-\mathrm{i}kz)P(-(\mathbf{v}-\mathbf{w}),z). \qquad (19)$$

Finally, let us calculate the FT of $b(\mathbf{r}'',z)$ using Eq. (2):

$$F_{\lambda z}[b(\mathbf{r}'',z)] = (\lambda z)^2 A(\alpha)\exp(\mathrm{i}k_z z)\delta(\sigma - r_1), \qquad (20)$$

where

$$r_1 = \frac{\lambda z}{r_0}. \qquad (21)$$

3.4. Fourth step

Now, we may write the FT of $s'(\mathbf{r}',\mathbf{w},z)$. After doing so, we will perform the inverse FT. Using Eqs. (19) and (20), we may write the FT of Eq. (15) as:

$$S'(\mathbf{v},\mathbf{w},z) = (\lambda z)^2 \exp(\mathrm{i}[k_z - k]z)P(-(\mathbf{v}-\mathbf{w}),z)$$
$$\times \delta(\sigma - r_1)A(\alpha). \qquad (22)$$

Performing the product of P with the delta function, we may write:

$$S'(\mathbf{v},\mathbf{w},z) = (\lambda z)^2 \exp(-\mathrm{i}kz)$$
$$\times P(u - r_1\cos\alpha, v - r_1\sin\alpha, z)A(\alpha)$$
$$\times \exp(\mathrm{i}k_z z)\delta(\sigma - r_1). \qquad (23)$$

This is our point-dependent (depends on $\mathbf{w}$ that will become $\mathbf{r}'$ after performing an inverse FT) pseudo-spectrum function. P is not a constant function and it changes the pseudo-spectrum in a different way for every $\mathbf{w}$. The last key point in our development is that the function $\exp(-\mathrm{i}kz)P(u - r_1\cos\alpha, v - r_1\sin\alpha)$ is a periodic function of α (period is 2π), and it may be expanded in a Fourier series:

$$\exp(-\mathrm{i}kz)P(u - r_1\cos\alpha, v - r_1\sin\alpha, z)$$
$$= \sum_{m=-\infty}^{\infty} c_m(\mathbf{w},z)\exp(\mathrm{i}m\alpha)$$
$$c_m(\mathbf{w},z) = \frac{\exp(-\mathrm{i}kz)}{2\pi}\int_0^{2\pi} P(u - r_1\cos\alpha, v - r_1\sin\alpha, z)$$
$$\times \exp(-\mathrm{i}m\alpha)\mathrm{d}\alpha \qquad (24)$$

In order to analyze the physical meaning of this expression it will be convenient to transform the expression of the functions $c_m(\mathbf{w},z)$. Defining $\beta = \alpha + \pi$ and using this in the integral, we obtain:

$$c_m(\mathbf{w},z) = \frac{(-1)^m \exp(-\mathrm{i}kz)}{2\pi}$$
$$\times \int_0^{2\pi} P(u + r_1\cos\beta, v + r_1\sin\beta, z)$$
$$\times \exp(-\mathrm{i}m\beta)\mathrm{d}\beta. \qquad (25)$$

This is the expression of $c_m(\mathbf{w},z)$ that we will use in what follows. Using Eq. (24) in Eq. (23), we obtain:

$$S'(\mathbf{v},\mathbf{w},z) = (\lambda z)^2 \sum_{m=-\infty}^{\infty} c_m(\mathbf{w},z)\exp(\mathrm{i}m\alpha)A(\alpha)$$
$$\times \exp(\mathrm{i}k_z z)\delta(\sigma - r_1). \qquad (26)$$

Performing the inverse FT:

$$s'(\mathbf{r'},\mathbf{w},z) = c_0(\mathbf{w},z)b(\mathbf{r'},z) + q(\mathbf{r'},\mathbf{w},z)$$

$$q(\mathbf{r'},\mathbf{w},z) = \sum_{m\neq0} c_m(\mathbf{w},z)k_r \exp(ik_z z)\int_0^{2\pi}\exp(im\alpha)A(\alpha)$$
$$\times \exp\left[ik_r r'\cos(\theta-\alpha)\right]\mathrm{d}\alpha \tag{27}$$

Finally, using $\mathbf{w}=\mathbf{r'}$ we may write:

$$s(\mathbf{r'},z) = c_0(\mathbf{r'},z)b(\mathbf{r'},z) + q(\mathbf{r'},z),$$

$$q(\mathbf{r'},z) = \sum_{m\neq0} c_m(\mathbf{r'},z)k_r \exp(ik_z z)\int_0^{2\pi}\exp(im\alpha)A(\alpha)$$
$$\times \exp\left[ik_r r'\cos(\theta-\alpha)\right]\mathrm{d}\alpha,$$

$$c_m(\mathbf{r'},z) = \frac{(-1)^m\exp(-ikz)}{2\pi}\int_0^{2\pi}P(x'+r_1\cos\beta,y'+r_1\sin\beta,z)$$
$$\times \exp(-im\beta)\mathrm{d}\beta. \tag{28}$$

Eq. (28) is the final result of our general analysis and will be discussed in the next sections. Note that the diffraction pattern of a SNB at any point $\mathbf{r'}$ may be written as the original NB $b(\mathbf{r'},z)$ modulated by a function $c_0(\mathbf{r'},z)$ that only depends on the characteristics of the diffraction of the pupil function; note that it corresponds to an average taken on a ring of radius r_1 of the diffraction pattern of the aperture centered at the point where the performance has to be evaluated. Also, a function $q(\mathbf{r'},z)$ has to be added. The function $q(\mathbf{r'},z)$ contains infinite terms. Every term is a product of a function $c_m(\mathbf{r'},z)$ times another function. The functions $c_m(\mathbf{r'},z)$ are the Fourier coefficients of the Fourier series expansion of the function $P(u-r_1\cos\alpha, v-r_1\sin\alpha)$; since this function will show in most cases a soft behavior, the functions $c_m(\mathbf{r'},z)$ will be negligible for high values of m. This means that a small number of terms will be needed to calculate $q(\mathbf{r'},z)$. This will be shown for several particular cases in Section 6. In all those cases it is shown that $q(\mathbf{r'},z)$ may be evaluated considering the terms corresponding to $m=-4,-3,\ldots,0,\ldots,3,4$.

Note that if $b(\mathbf{r'},z)$ is a Bessel function of order n, then $q(\mathbf{r'},z)$ may be written as a linear combination of Bessel functions. For an n-order Bessel beam we may use the definition of A given in Eq. (3) into Eq. (28) to obtain:

$$s(\mathbf{r'},z) = c_0(\mathbf{r'},z)J_n\left(2\pi\frac{r'}{r_0}\right)\exp(in\theta)$$
$$\times \exp(ik_z z) + q(\mathbf{r'},z),$$

$$q(\mathbf{r'},z) = \sum_{m\neq0}i^m c_m(\mathbf{r'},z)J_{m+n}\left(2\pi\frac{r'}{r_0}\right)$$
$$\times \exp\left[i(m+n)\theta\right]\exp(ik_z z). \tag{29}$$

We may then notice from Eqs. (28) and (29) that the numerical design of DE [40] and the numerical calculation of apodization functions [41] to obtain SNBs with certain properties may be now reduced to the calculation of convenient pupils which generates convenient diffraction patterns. Also, those expressions may allow a simple analysis of the disturbance on the orbital angular momentum distribution of the beam [23] generated by the aperture or for the presence of an obstacle.

3.5. Rotationally symmetric aperture

In some experimental setups, the pupil function may be rotationally symmetric. For this particular case the expressions that we have just developed may be slightly simplified. Let us use cylindrical coordinates in the definition of the functions $c_m(\mathbf{r'},z)$ in Eq. (28):

$$c_m(\mathbf{r'},z) = \frac{(-1)^m\exp(-ikz)}{2\pi}$$
$$\times \int_0^{2\pi}P(r'\cos\theta+r_1\cos\beta,r'\sin\theta+r_1\sin\beta,z)$$
$$\times \exp(-im\beta)\mathrm{d}\beta. \tag{30}$$

If P is rotationally symmetric, this implies that it only depends on the magnitude of the position vector of the point where we wish to evaluate P. Then, we may write:

$$c_m(\mathbf{r'},z) = \frac{(-1)^m\exp(-ikz)}{2\pi}$$
$$\times \int_0^{2\pi}P\left(\sqrt{r'^2+r_1^2+2r'r_1\cos(\beta-\theta)},z\right)$$
$$\times \exp(-im\beta)\mathrm{d}\beta. \tag{31}$$

Using a new variable $\delta=\beta-\theta$, we obtain:

$$c_m(\mathbf{r'},z) = \exp(-im\theta)d_m(\mathbf{r'},z), \tag{32}$$

where

$$d_m(\mathbf{r}',z) = \frac{(-1)^m \exp(-ikz)}{2\pi}$$
$$\times \int_0^{2\pi} P\left(\sqrt{r'^2 + r_1^2 + 2r'r_1\cos(\delta)}, z\right)$$
$$\times \exp(-im\delta)\mathrm{d}\delta. \qquad (33)$$

Note that $c_0(\mathbf{r}',z) = d_0(\mathbf{r}',z)$. Let us use all this for the particular case of an n-order Bessel beam in Eq. (29):

$$s(\mathbf{r}',z) = c_0(\mathbf{r}',z)J_n\left(2\pi\frac{r'}{r_0}\right)\exp(in\theta)$$
$$\times \exp(ik_zz) + q(\mathbf{r}',z)\exp(in\theta),$$
$$q(\mathbf{r}',z) = \sum_{m\neq0} i^m d_m(\mathbf{r}',z)J_{m+n}\left(2\pi\frac{r'}{r_0}\right)\exp(ik_zz).$$
$$(34)$$

Finally, for the particular case of a J_0:

$$s(\mathbf{r}',z) = e_0(\mathbf{r}',z)J_0\left(2\pi\frac{r'}{r_0}\right)\exp(ik_zz) + q(\mathbf{r}',z),$$
$$q(\mathbf{r}',z) = \sum_{m=1}^{\infty} i^m e_m(\mathbf{r}',z)J_m\left(2\pi\frac{r'}{r_0}\right)\exp(ik_zz),$$
$$e_0(\mathbf{r}',z) = d_0(\mathbf{r}',z)$$
$$e_{m\neq0}(\mathbf{r}',z) = d_m(\mathbf{r}',z) + d_{-m}(\mathbf{r}',z).$$
$$(35)$$

Note that $e_0(\mathbf{r}',t) = d_0(\mathbf{r}',t) = c_0(\mathbf{r}',t)$. Those expressions will be used to obtain numerical results shown in several figures.

In the following sections, we are going to analyze and illustrate the physical meaning of the expressions we have derived. Eq. (28) shows that the functions $c_m(\mathbf{r}',z)$ depends only on the characteristics of the diffraction pattern of the pupil function. The pupil function depends on the setup used to generate the SNB. For the sake of simplicity, we will consider a circular aperture of radius R. Then, in the next section, we study certain characteristics of the diffraction pattern of a circular aperture that will be useful for the discussion of the performance of the SNB in Sections 5 and 6.

4. Diffraction pattern of a circular aperture

The diffraction pattern of a circular aperture is a very well known pattern that may be easily

characterized by N_F as commented in Section 2. For the cases of experimental interest the diffraction pattern of the pupil will correspond to a near field diffraction pattern. This is not a condition for the validity of our development but in our examples we will consider $N_F > 10$.

The near field diffraction pattern of a circular aperture is rotationally symmetric and it looks like a set of $N_F/2$ concentric light rings separated by dark rings. Then, in the transverse amplitude profile, the number of maxima and minima increase as N_F increases, but the amplitude of the oscillations decreases (in the Fresnel integral, for $N_F \to \infty$, we recover the aperture function). Ignoring the behavior in the points close to the optical axis, the frequency of the oscillations becomes slower as we increase the radial coordinate r' and the amplitude of the oscillations become stronger. Some of those characteristics may be observed in Fig. 1, where the transverse amplitude profile for two different values of $N_F = 12.64$ and 31.60 are represented. Those Fresnel numbers may correspond to the diffraction of a circular aperture with $R = 2$ cm, $\lambda = 632.8$ nm (He–Ne laser) at the distances $z = 50$ and 20 m.

The behavior of the diffraction pattern of the aperture around the geometrical projection of the edge of the aperture will be important in order to describe the performance of $s(\mathbf{r}',z)$ when z is near the maximum propagation distance. Then, we are going to develop an expression that allows us to analyze the characteristics of this diffraction pattern around this region. We may expect that the diffraction of a circular aperture will behave as a first approximation as the diffraction of a sharp edge [42] for the coordinate r'. This implies two basic facts [42]: (i) there is a an absolute maximum of the amplitude near to the geometrical projection of the edge; (ii) the intensity for the points corresponding to the geometrical projection of the edge is reduced to one quarter of the corresponding intensity for an infinite aperture.

We consider then the diffraction pattern at the coordinates ($x' = r'$, $y = 0$) for r' around the geometric projection of the edge of the aperture, and we will assume that we may approximate the Fresnel diffraction integral of the aperture as follows:

$$P(r',z) \simeq \frac{\exp(\mathrm{i}kz)}{\mathrm{i}\lambda z} \int_{-\infty}^{+\infty} \exp\left(\frac{\mathrm{i}\pi}{\lambda z}y^2\right)\mathrm{d}y$$

$$\times \int_{-\infty}^{R} \exp\left(\mathrm{i}\frac{\pi}{\lambda z}(x-r')^2\right)\mathrm{d}x. \tag{36}$$

Using the following variable $\eta_r = (2/(\lambda z))^{1/2}$ $(x - r')$ in Eq. (36), we obtain:

$$P(r',z) \simeq \exp(\mathrm{i}kz)\left[\frac{1}{2} + \frac{\sqrt{2}}{2}\exp\left(-\mathrm{i}\frac{\pi}{4}\right)(C(\eta_R) + \mathrm{i}S(\eta_R))\right], \tag{37}$$

where

$$\eta_R = \sqrt{\frac{2}{\lambda z}}(R - r'), \tag{38}$$

and $C(\eta_R)$ and $S(\eta_R)$ are the real and imaginary parts of the Fresnel integral [36]. The amplitude of $P(r',z)$ takes its maximum value for $\eta_R = 1.22$ (this has been established by numerical calculation). Solving Eq. (38) for r' and denoting r'_m the position of the maximum we obtain:

$$r'_m = R - 0.855\sqrt{\lambda z}, \tag{39}$$

and the maximum value of the amplitude is:

$$|P(r'_m, z)| \simeq 1.17. \tag{40}$$

This means that the intensity at $r = r_m$ is about 37% higher than for the case of an infinite aperture. For our development it is also important to calculate the amplitude for $r' = R$:

$$|P(R,z)| \simeq 0.5. \tag{41}$$

This means that the intensity for $r'_m = R$ is a 75% lower than for the case of an infinite aperture.

5. Amplitude distribution on the optical axis

In this section and in the next section, we are going to analyze the physical meaning of the expressions we have derived in Section 3 and we are going to illustrate them with several examples. In this section, we will discuss the performance on the optical axis using the results of Section 4. First, let us analyze the modulating function $c_0(\mathbf{r}' = 0, z)$ for an arbitrary pupil. From Eq. (28) it may be written as follows:

$$c_0(0,z) = \frac{\exp(-\mathrm{i}kz)}{2\pi} \int_0^{2\pi} P(r_1\cos\beta, r_1\sin\beta)\mathrm{d}\beta. \tag{42}$$
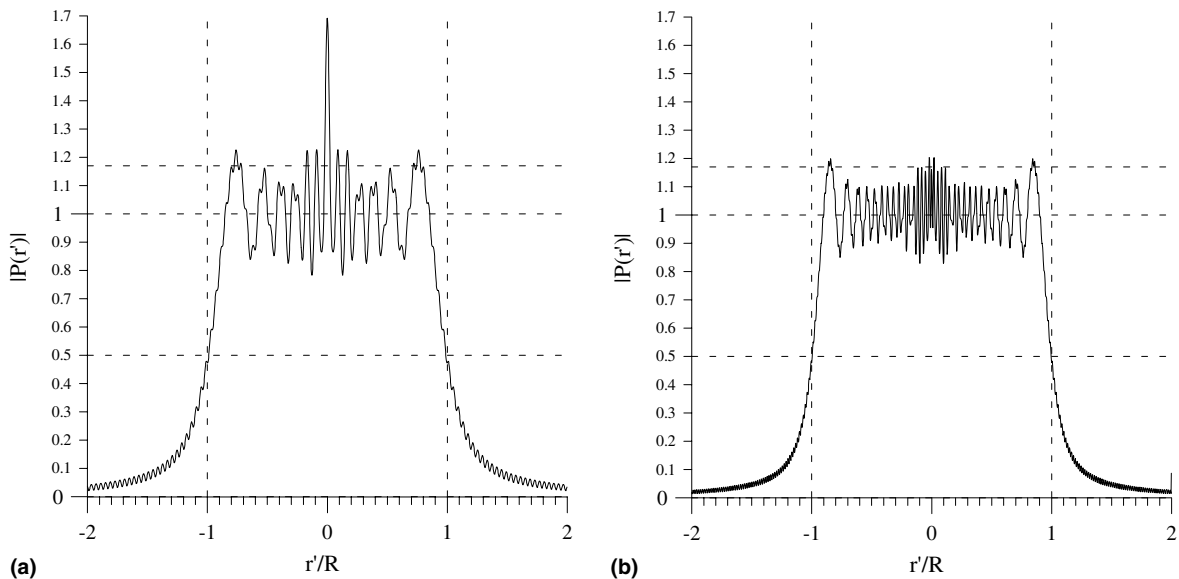

Fig. 1. Transverse amplitude distribution of the diffraction pattern of a circular aperture for: (a) $N_F = 12.64$ and (b) $N_F = 31.60$.

The meaning of this function is very simple: $c_0(0,z)$ is the average value of the diffraction pattern of the aperture on a ring of radius r_1 centered at the optical axis (affected by a factor $\exp(-ikz)$, that will cancel with the factor $\exp(ikz)$ contained in the Fresnel diffraction formula in Eq. (5)).

If P is rotationally symmetric, then it shows a constant value on the ring. From Eq. (28), this fact implies that the other functions $c_m(0,z) = 0$ for $m \neq 0$; then $q(0,z) = 0$ on the optical axis. We conclude that the complex amplitude on the optical axis for a circular aperture (or any aperture which is rotationally symmetric) may be exactly written as:

$$s(0,z) = c_0(0,z)b(0,z). \tag{43}$$

From Eq. (29), note that for the J_0 beam, Eq. (43) may be also used even if the aperture is not rotationally symmetric, because higher order Bessel beams have a zero on the optical axis.

Let us continue our discussion assuming that the pupil function is a circular aperture. We will follow several steps that should be followed in a similar way for any other definition of the pupil function, but taking into account the specific properties of the diffraction pattern generated by the pupil function. From the shape of the diffraction pattern of a circular aperture we may easily predict the qualitative behavior of $c_0(\mathbf{r}',z)$ as we increase z from three basic facts: (i) the radius of the ring r_1 increases as z increases, (ii) the number of maxima and minima of the diffraction pattern of the aperture decreases (the frequency of the oscillations decreases) because N_F decreases as z increases, (iii) the amplitude of the oscillations of the diffraction pattern of the aperture increase with z because N_F decreases as z increases. Then, the ring will lie on consecutive maxima and minima: $c_0(\mathbf{r}',z)$ will show an oscillatory behavior as z increases and the amplitude of those oscillations will increase and the frequency will decrease. When the ring lies on the last maximum of the diffraction pattern of the circular aperture, $c_0(0,z)$ will have reached its last maximum. We denote z_m the position of this last maximum. This is a important maximum because it is an absolute maximum near the maximum propagation distance, as we shall see. z_m

may be calculated using $r'_m = r_1$ in Eq. (39) and the definition of r_1 in Eq. (21) to obtain:

$$R - \frac{\lambda z_m}{r_0} = 0.855\sqrt{\lambda z_m}. \tag{44}$$

Solving for z_m and considering $R/r_0 \gg 1$:

$$z_m = \frac{R r_0}{\lambda}\left(1 - 0.855\sqrt{\frac{r_0}{R}} + 0.265 \cdot \frac{r_0}{R}\right). \tag{45}$$

From Eq. (40), we may write:

$$|c(0,z_m)| \simeq 1.17. \tag{46}$$

For $z > z_m$ the ring lies on a region where the amplitude monotonically decrease, then $c_0(\mathbf{r}',z)$ also monotonically decreases. In this region, for a certain distance that we will denote as z_D, the ring achieves a radius equal to the radius of the circular aperture. Using Eq. (21) and $r_1 = R$, we obtain:

$$z_D = \frac{R r_0}{\lambda}, \tag{47}$$

and using Eq. (41), we may write:

$$|c_0(0,z_D)| \simeq 0.5, \tag{48}$$

z_D is known as the maximum distance of propagation for the J_0 beam when a circular aperture is used and it was first defined from arguments based on geometrical optics [2].

All those results are illustrated in Fig. 2, where the amplitude of $c_0(0,z)$ (calculated with Eq. (33)) is represented as a function of z/z_m (z_m is calculated using Eq. (45)) for five cases, $R/r_0 = 10, 20, 50, 100, 200$; the last z considered for every case is z_D. It is interesting to note that $N_F = R/r_0$ for $z = z_D$. We may see that z_m and z_D become very close distances for $R/r_0 \gg 1$. This can be also easily concluded using Eq. (47) in Eq. (45):

$$z_m = z_D\left(1 - 0.855\sqrt{\frac{r_0}{R}} + 0.265 \cdot \frac{r_0}{R}\right). \tag{49}$$

In the figures we may observe that the maximum value tends to be 1.17 as predicted in Eq. (46). Also note that for $z = z_D$ the amplitude tends to be 0.5 as predicted in Eq. (48). As we may see in Fig. 2, Eq. (49) is highly accurate even for low values of N_F. We will consider again the distance z_m when we deal with long-range NBs in Section 7.

Fig. 2 shows also the accuracy of the "straight edge" approximations performed in the last section. It was first noted by Durning [1] the similarity of the behavior of a SNB on the optical axis with the Fresnel diffraction pattern of a straight edge.

6. Transverse amplitude distribution

As in the last section, we start by studying $c_0(\mathbf{r}',z)$. Its physical meaning is simple. From Eq. (28), $c_0(\mathbf{r}',z)$ corresponds to the average of the diffraction pattern P at a distance z on a ring of radius r_1 centered at the coordinates $\mathbf{r}'$. $c_0(\mathbf{r}',z)$ acts as a modulating function of the NB $b(\mathbf{r}',z)$.

Let us consider P a circular aperture. The ring will be lying on several maxima and minima of the diffraction pattern. If we consider $c_0(\mathbf{r}',z)$ for a certain z, we may expect that as r' increases from zero, $c_0(\mathbf{r}',z)$ should oscillate around unity. For $r' > R - r_1$, the ring will start lying outside the geometrical projection of the aperture and the amplitude of $c_0(\mathbf{r}',z)$ will start to decrease. For $r' = R$ the center of the ring lies at the edge
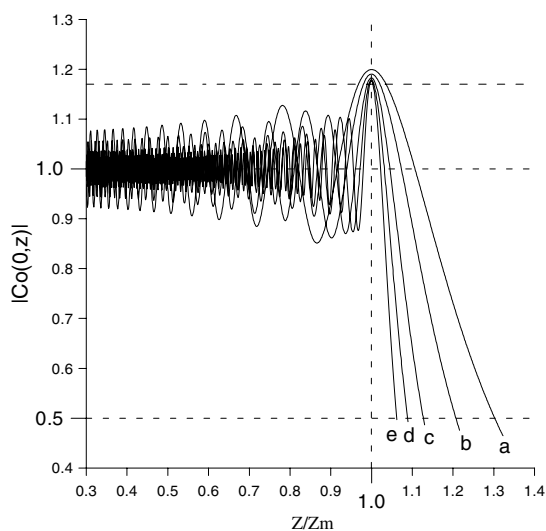

Fig. 2. Magnitude of the amplitude of $c_0(0,z)$ as a function of z/z_m for (a) $R/r_0 = 10$, (b) $R/r_0 = 20$, (c) $R/r_0 = 50$, (d) $R/r_0 = 100$, (e) $R/r_0 = 200$. The upper dashed line corresponds to $c_0(0,z) = 1.17$.

of the geometrical projection of the aperture, so $c_0(\mathbf{r}',z) < 0.5$. For $r' \geqslant R + r_1$ we expect a negligible value for $c_0(\mathbf{r}',z)$.

In order to describe the performance of the SNB for $r' > 0$ the functions $c_m(\mathbf{r}',z)$ for $m \neq 0$ have to be also considered. Those functions appeared from a Fourier Series development of a periodic function (the function P on a ring of radius r_1 centered at $\mathbf{r}'$) in Eq. (24) and should show the same properties of any Fourier coefficients. Then $c_m(\mathbf{r}',z)$ will take values different from zero if P is not a constant function on the ring. This may happen for two reasons in two different cases:

(i) The ring lying inside the geometric projection of the aperture ($r' < R - r_1$): In this case P will not be a constant function because the diffraction pattern behaves as an oscillatory complex function and the amplitude consists on a set of concentric maxima and minima. For low Fresnel numbers we expect the coefficients $c_m(\mathbf{r}',z)$ to have a non-negligible (but not strong) contribution to the distortion of the diffraction pattern of the SNB. As higher Fresnel numbers are considered, the amplitude of the oscillations are smaller and the functions $c_m(\mathbf{r}',z)$ for $m \neq 0$ will become smaller.

(ii) The ring having a section lying outside the geometric projection of the aperture ($R - r_1 < r' < R + r_1$): Then a sector of the ring will lie on a region where P takes very low values: this implies a much stronger variation of P on the ring. This fact is very important and it will make the functions $c_m(\mathbf{r}',z)$ to take larger values than in case (i). Then we expect a very important distortion of the diffraction pattern for $r' > R - r_1$. For $r' > R + r_1$ the functions $c_m(\mathbf{r}',z)$ should have negligible values.

From (i) and (ii), if the diffraction pattern of the aperture corresponds to a large Fresnel number it is possible to derive an analytical asymptotic approximation of the functions $c_m(\mathbf{r}',z)$. This is done in Appendix A. When the diffraction pattern of the aperture corresponds to lower Fresnel

numbers we expect the functions $c_m(\mathbf{r}',z)$ only to follow approximately their asymptotic behavior in case (ii), because the main contribution to function $c_m(\mathbf{r}',z)$ should come from the finite size of the diffraction pattern of the aperture. Comparisons of those asymptotic values and the real ones will be shown in several figures.

All this discussion obviously applies to the functions in $d_m(\mathbf{r}',z)$ defined in Eq. (33) and the functions $e_m(\mathbf{r}',z)$ defined in Eq. (35) as well.

The performance of the SNB will also strongly depend on r_1, the radius of the ring. In the next sections we will discuss the transverse amplitude distribution of the diffraction pattern of a J_0 beam generated with a circular DE in four representative cases, $r_1/R \ll 1$, $r_1/R \approx 0.5$, $r_1/R = r'_m/R < 1$ and $r_1/R = 1$ (equivalent to $z = z_D$), and for every case we will consider the Fresnel numbers used in Fig. 1. In every case, we will choose a certain value for N_F and for r_1/R, then r_0 may be easily calculated using Eqs. (4) and (21): $r_0/R = R/r_1 N_F$. The graphical representations for each case correspond to Figs. 3–6. Every figure will be discussed in a different section. For every case, we show a comparison of the amplitude distribution corresponding to: (i) Exact calculation using the Fresnel diffraction integral in Eq. (5), (ii) Calculation using our development (Eq. (35)) with the following approximation:

$$s(\mathbf{r}',z) \simeq e_0(\mathbf{r}',z) J_0\left(2\pi \frac{r'}{r_0}\right) \exp(\mathrm{i}k_z z)$$
$$+ \sum_{m=1}^{4} \mathrm{i}^m e_m(\mathbf{r}',z) J_m\left(2\pi \frac{r'}{r_0}\right) \exp(\mathrm{i}k_z z).$$
$$(50)$$

We do this in order to show the high convergence of our development (for most cases (i) and (ii) are undistinguishable), and (iii) calculation for an infinite aperture; this way we will observe the modulation or distortion due to the diffraction effects suffered by the SNB. Also the amplitude of $e_m(\mathbf{r}',z)$ for $m = 0$, 1, 2 are represented for each case in order to justify the shape of the transverse amplitude distributions and in several figures (the ones that contain a important interval for $r' > R - r_1$) we represent also the asymptotic functions derived in Appendix A.

6.1. $r_1/R \ll 1$

In this case $e_0(\mathbf{r}',z)$ corresponds to an average value performed in a small ring. Taking into account the shape of the transverse amplitude distributions of the diffraction pattern of the aperture shown in Fig. 1, we expect $e_0(\mathbf{r}',z)$ to behave as an oscillating function for $r' < r'_m$ and to have approximately the same number of maxima and minima than the diffraction pattern of the aperture. We expect also that for $r' > r'_m e_0(\mathbf{r}',z)$ should show a decrease that corresponds to the diffraction pattern of the aperture. Those oscillations and the final decrease will modify in a non-negligible way the shape of the NB. The higher the Fresnel number of the aperture, the lower those oscillations should be. The functions $e_m(\mathbf{r}',z)$ for $m \neq 0$, should take non-negligible values for $r' < r'_m$ (because the noticeable oscillation of the diffraction pattern of the aperture) and also we expect them to be more important for lower Fresnel numbers. For $r' > r'_m$ the ring lies in a region where the amplitude of the diffraction pattern shows a very steep decrease, then the functions $e_m(\mathbf{r}',z)$ for m an odd integer, clearly should raise in this region. We may illustrate all this in Fig. 3, where we consider two different cases (i) $N_F = 12.64$, $r_1/R = 0.0880$ and $r_0/R = 0.899$; (ii) $N_F = 31.60$, $r_1/R = 0.0820$, $r_0/R = 0.386$. For both cases: (i) the ring lies on a maximum of the diffraction pattern of the aperture for $r' = 0$; (ii) the scale factor for J_0 is big and the oscillations of $e_0(\mathbf{r}',z)$ are fast. Then we observe a distorted J_0 rather than a modulated J_0.

In this case the ring is very small, and the functions are highly sensitive to the characteristics of the diffraction pattern of the aperture. The interval of points that verify $r' > R - r_1$ is very small. Then, we may expect no agreement between the functions $e_m(\mathbf{r}',z)$ and the corresponding asymptotic values and they are not represented.

6.2. $r_1/R \approx 0.5$

In this case, the integral that define the function $e_0(\mathbf{r}',z)$ is performed on a larger ring, so we expect the amplitude of the oscillations to be smaller and because the ring is closer to the edge, we expect the oscillations to be slower (As one may see from
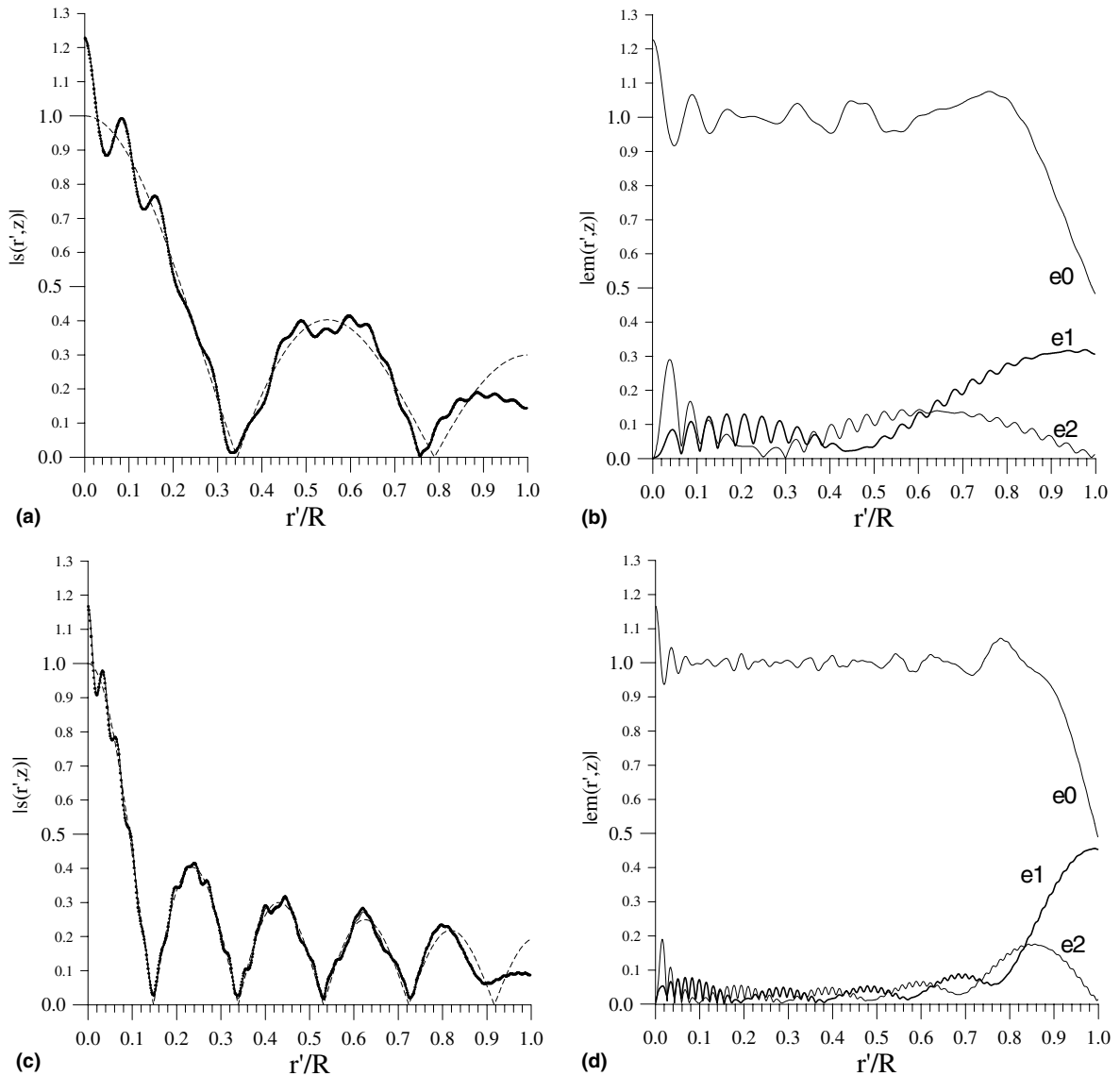
Fig. 3. Transverse amplitude distribution corresponding to a J_0 and graphical representation of three of the functions $e_m(r',z)$ for two cases: figures (a) and (b) correspond to: $N_F = 12.64$, $r_1/R = 0.0880$, $r_0/R = 0.899$; figures (c) and (d) correspond to: $N_F = 31.60$, $r_1/R = 0.0820$, $r_0/R = 0.386$. In figures (a) and (c) dashed line corresponds to a perfect J_0 function, continuous line corresponds to an exact calculation with the Fresnel diffraction integral, dotted line corresponds to an approximation using four terms. In figures (b) and (d) the function e_1 has been represented with a thicker line.

Fig. 1 the oscillations of the diffraction pattern are slower as more close they are from the geometrical projection of the edge of the aperture).

In this case, the scale of J_0 is reduced. Then, we expect to observe a modulated J_0 (stronger modulation for lower Fresnel number) instead of a distorted J_0 as in Fig. 3. To illustrate this, we consider two examples in Fig. 4: (i) $N_F =$ 12.64, $r_1/R = 0.52$, $r_0/R = 0.152$; (ii) $N_F = 31.60$, $r_1/R = 0.478$, $r_0/R = 0.066$. For both cases: (i)
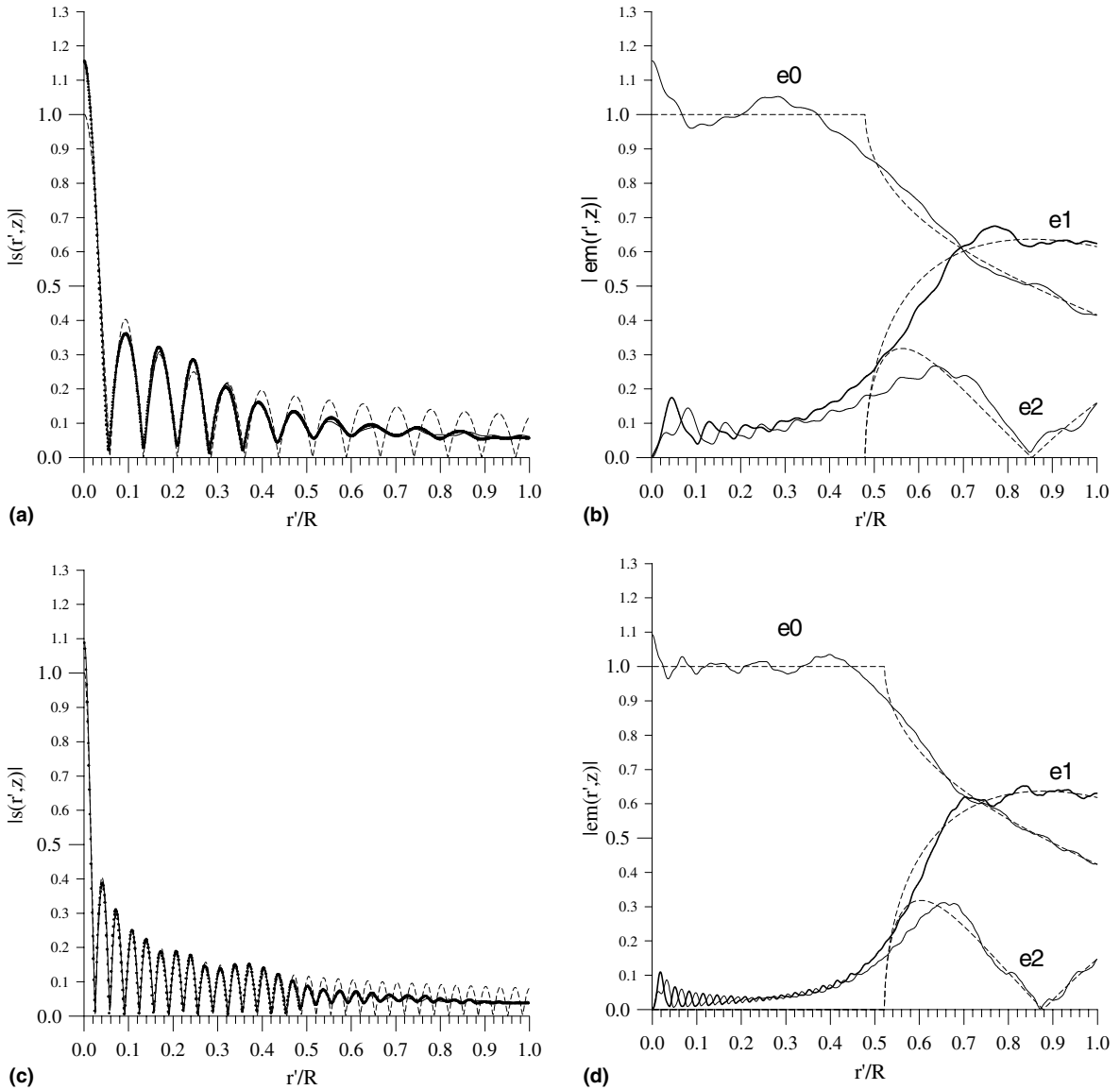
Fig. 4. Transverse amplitude distribution corresponding to a J_0 and graphical representation of three of the functions $e_m(r',z)$ for two cases: figures (a) and (b) correspond to: $N_F = 12.64$, $r_1/R = 0.52$, $r_0/R = 0.152$; figures (c) and (d) correspond to: $N_F = 31.60$, $r_1/R = 0.478$, $r_0/R = 0.066$. In figures (a) and (c) dashed line corresponds to a perfect J_0 function, continuous line corresponds to an exact calculation with the Fresnel diffraction integral, dotted line corresponds to an approximation using four terms. In figures (b) and (d) the function e_1 has been represented with a thicker line and the dashed line corresponds to the asymptotic approximation for each function.

the ring lies on a maximum of the diffraction pattern of the aperture when it is centered on the optical axis. (ii) For $r' > R - r_1$, the ring lies outside the geometrical projection of the aper-ture, and in the graphics, one may observe that in this region $e_0(\mathbf{r}',z)$ decreases and the other function $e_m(\mathbf{r}',z)$ raise and follow a behavior close to their asymptotic values. Then for
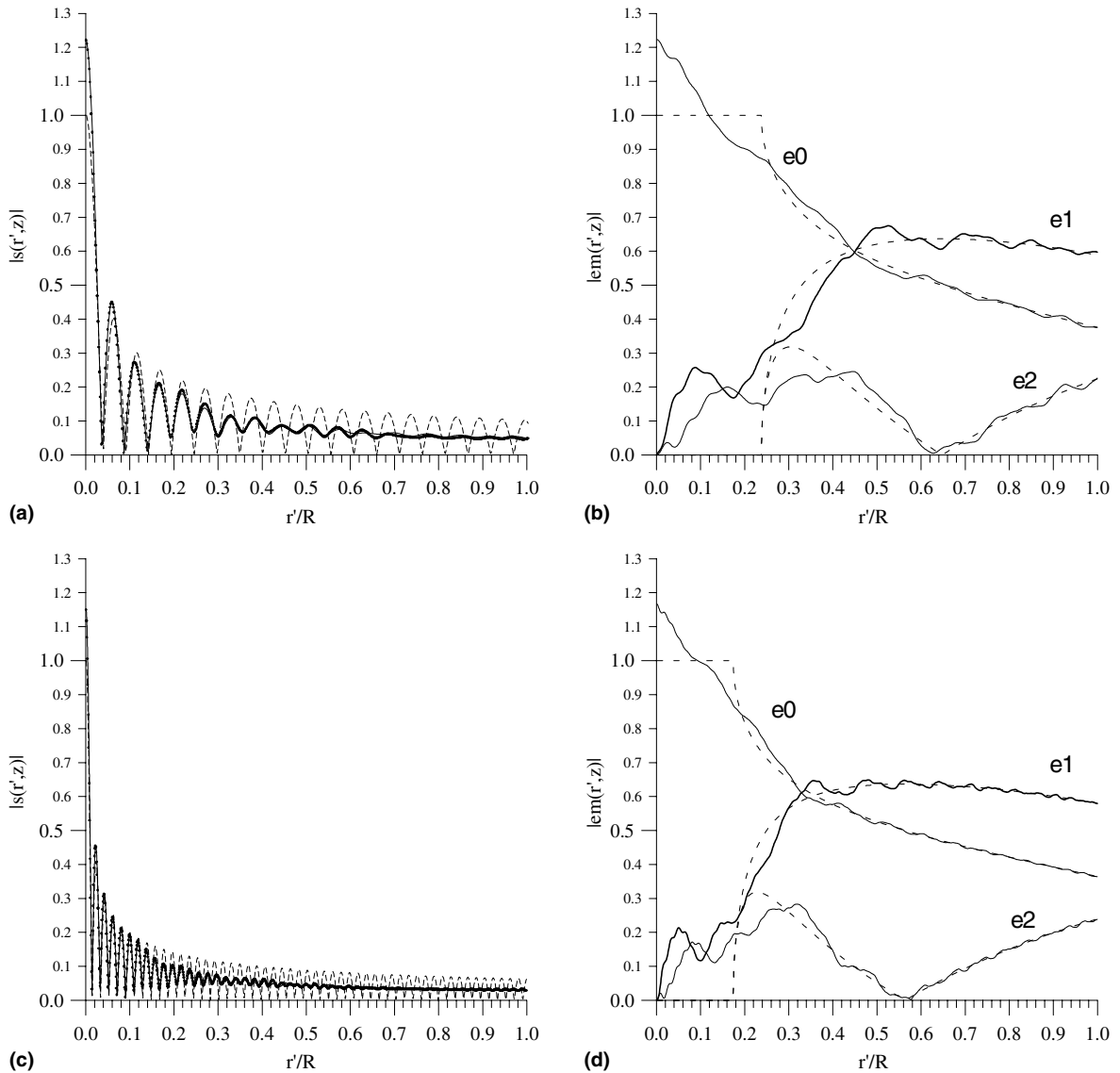
Fig. 5. Transverse amplitude distribution corresponding to a J_0 and graphical representation of three of the functions $e_m(r',z)$ for two cases: figures (a) and (b) correspond to: $N_F = 12.64$, $r_1/R = 0.762$, $r_0/R = 0.1035$; figures (c) and (d) correspond to: $N_F = 31.60$, $r_1/R = 0.826$, $r_0/R = 0.0383$. In figures (a) and (c) dashed line corresponds to a perfect J_0 function, continuous line corresponds to an exact calculation with the Fresnel diffraction integral, dotted line corresponds to an approximation using four terms. In figures (b) and (d) the function e_1 has been represented with a thicker line and the dashed line corresponds to the asymptotic approximation for each function.

$r' > R - r_1$ the performance of the J_0 worsens: the oscillations of J_0 decreases and finally takes a value that seems to correspond to an average value of the former oscillations. This may be also observed in Figs. 5 and 6.

6.3. $r_1/R = r'_m/R$

In this case the ring lies on the last maximum of the diffraction pattern of the aperture when it is centered on the optical axis; from Eq. (44) this will
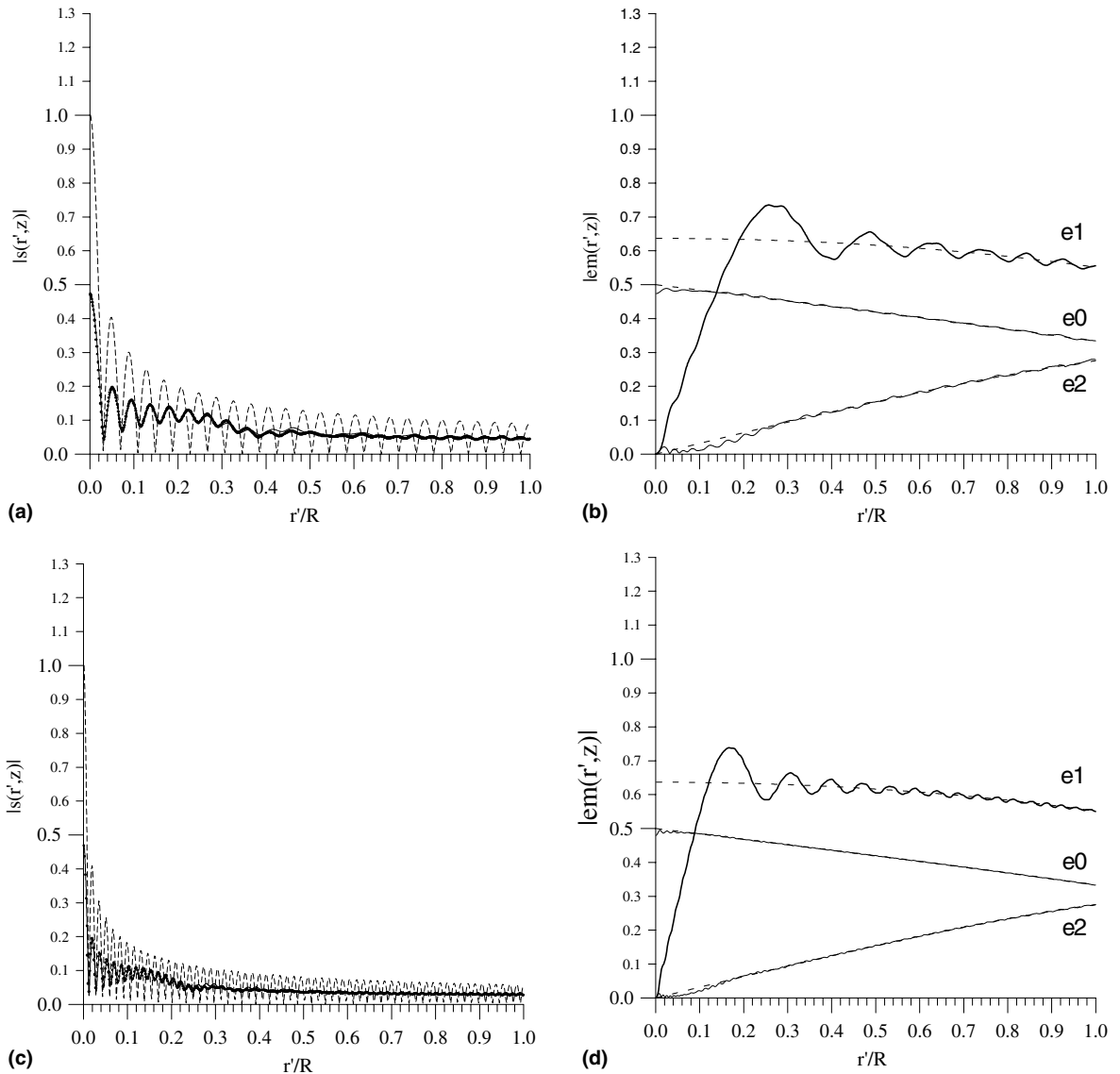
Fig. 6. Transverse amplitude distribution corresponding to a J_0 and graphical representation of three of the functions $e_m(r',z)$ for two cases: figures (a) and (b) correspond to: $N_F = 12.64$, $r_1/R = 1$, $r_0/R = 0.0791$; figures (c) and (d) correspond to: $N_F = 31.60$, $r_1/R = 1$, $r_0/R = 0.03164$. In figures (a) and (c) dashed line corresponds to a perfect J_0 function, continuous line corresponds to an exact calculation with the Fresnel diffraction integral, dotted line corresponds to an approximation using four terms. In figures (b) and (d) the function e_1 has been represented with a thicker line and the dashed line corresponds to the asymptotic approximation for each function.

happen for $r_1/R = r'_m/R = 1 - 0.855/N_F^{1/2}$. Then in Fig. 5, two cases are considered: (i) $N_F = 12.64$, $r_1/R = 0.762$ and $r_0/R = 0.1035$; (ii) $N_F = 31.60$ and $r_1/R = 0.826$ and $r_0/R = 0.0383$ (Note that the scale factor for J_0 is now still smaller). For this case we observe that $e_0(r',z)$ shows a continuous decrease

in its value because the ring, initially centered at the optical axis, was at the maximum of the diffraction pattern of the aperture and near the geometrical projection of the edge of the aperture. This continuous decrease modulates J_0. The other functions $e_m(r',z)$ follow a closer behavior to the

asymptotic values for $r' > R - r_1$, which implies a complete distortion of the performance of the SNB in that region. Note that in this case, there are smaller differences for different Fresnel numbers. The reason for this is that the behavior of the diffraction pattern near the geometrical projection of the edge of the aperture does not show important differences for different Fresnel numbers as may be concluded from Section 4; the only important difference is a scale factor that depends on N_F.

6.4. $r_1/R = 1$

This case corresponds to $z = z_D$. Two examples are considered in Fig. 6: (i) $N_F = 12.64$, $r_1/R = 1$, and $r_0/R = 0.0791$, (ii) $N_F = 31.60$, $r_1/R = 1$, $r_0/R = 0.03164$. The function $e_0(\mathbf{r}',z)$ has a value near to 0.5 (as predicted in Eq. (48)) in the optical axis and it softly decays as we consider higher values of r'. In this case the modulating effect of $e_0(\mathbf{r}',z)$ is small. The diffraction pattern of the Bessel beam will then be highly distorted because the condition $r' > R - r_1$ becomes $r' > 0$; this condition is evidently fulfilled for any r' and then $e_m(\mathbf{r}',z)$ take important values even near the optical axis. Note that the behavior of the Bessel beams and the functions $e_m(\mathbf{r}',z)$ is almost the same for both cases; the only difference is a scale factor as already noted in Section 6.3. The functions $e_m(\mathbf{r}',z)$ show a behavior still closer to the asymptotic values; the exception is $e_1(\mathbf{r}',z)$ near the optical axis.

We have then shown that the appearance of any SNB can be predicted or justified from the shape of the diffraction pattern of the aperture and from the size and shift of the ring. In the figures a J_0 beam has been considered but the discussion and the results applies on general NBs generated with the same aperture (note that the functions $e_m(\mathbf{r}',z)$ do not have any dependence with the SNB being generated).

7. Long range SNBs

The maximum propagation distance of a certain SNB may be too small for a certain optical application. When this happens, one possible solu-

tion is to illuminate the DE with a divergent spherical wave [12] or to encode it in the DE. In this way, we may increase the diffraction range obtaining a long range divergent SNB [27]. We will now calculate the complex amplitude distribution in such a case.

If a spherical wave with origin at a distance d from the DE illuminates the DE, the complex amplitude distribution may be written, using Eq. (5), as:

$$s_d(\mathbf{r}',z) = \frac{\exp(ikz)}{\lambda z} \int \int t(\mathbf{r}) \exp\left(\frac{ik}{2d}\mathbf{r}^2\right) \\ \times \exp\left(\frac{ik}{2z}[\mathbf{r}' - \mathbf{r}]^2\right) dx\, dy, \qquad (51)$$

where the convolution is explicitly written. Defining $M = (d + z)/d$ and using it in Eq. (51), we obtain:

$$s_d(\mathbf{r}',z) = \frac{1}{M} \exp\left(ik\frac{z^2}{d+z}\right) \\ \times \exp\left(\frac{ik}{2(z+d)}\mathbf{r}'^2\right) s\left(\frac{\mathbf{r}'}{M},\frac{z}{M}\right). \qquad (52)$$

Thus we have exactly the same light distribution at z as we had before at $z/M = zd/(z + d)$, but affected by a scale factor given by M. Then, the maximum distance of propagation becomes $z'_D = dz_D/(d - z_D)$.

If we wish the range to be infinite and we consider a circular aperture as a pupil, we may propose to use $d = z_m$ instead of z_D, for three reasons: (i) $|c_0(0,0,z_m)|^2/|c_0(0,0,z_D)|^2$ is about 5.5, (ii) both distances are very similar as it was shown by means of Eq. (49), (iii) the performance is better at $z = z_m$. Note that (i) and (iii) are important if we are considering a long range or even an infinite range of propagation because atmospheric turbulences may affect intensity and performance. Then assuming $d = z_m$ for $z \to \infty$, we may write the complex amplitude distribution as:

$$s_f(\mathbf{r}',z) = \frac{1}{z} \exp(ikz) \exp\left(\frac{ik}{2z}\mathbf{r}'2\right) s\left(\frac{z_m}{z}\mathbf{r}',z_m\right). \qquad (53)$$

Note that the far field diffraction pattern corresponds to the one for $z = z_m$ when the DE was illuminated by a plane wave, but with a scale factor

z/z_m. Note that the intensity of this "diverging SNB" will decay as $(1/z)^2$ as any far field diffraction pattern.

8. Conclusions

A diffraction theory based on Fresnel diffraction has been developed in order to evaluate the performance of a SNB generated with an arbitrary finite-aperture system. We have shown the following:

(i) The Fresnel diffraction integral may be exactly solved in terms of the diffraction pattern of the aperture of the system. This has been done by transforming the Fresnel diffraction integral and then defining a convenient 5-dimensional function. The Fourier Transform of this function is simple and defines a point-dependent pseudo-spectrum function. The simplicity of this function allows to develop a meaningful analytical analysis.

(ii) The solution we have found out contains the original infinite-extent nondiffracting beam affected by a modulating function. This modulating function does not depend on the nondiffracting beam being generated and it corresponds to an average taken on a ring of the diffraction pattern of the aperture centered at the point where the performance has to be evaluated. This ring has a radius proportional to the wavelength and the distance from the aperture and is inversely proportional to a scale factor of the nondiffracting beam. The solution also contains additive functions that become important when the ring has a section lying outside the geometrical projection of the aperture. Then, the performance of a SNB may be justified or predicted from the characteristics of the diffraction pattern of the aperture of the system that generates the SNB and the size and shift of the ring.

(iii) We have studied the J_0 beam diffracted by a circular aperture and we have shown that its characteristics may be easily understood from the properties of the diffraction pattern of a circular aperture. The results apply to a general nondiffracting beam generated with the same aperture.

(iv) This theoretical development is useful to describe nondiffracting X and Y beams, because they are a superposition of NBs with different frequencies.

(v) The numerical design of DE [40] and the numerical calculation of apodization [41] functions to obtain SNBs with certain properties may be now reduced to the calculation of convenient pupils which generates convenient diffraction patterns.

(vi) Our theoretical results may allow a simple analysis of the disturbance on the orbital angular momentum distribution of the beam [23] generated by the aperture or for the presence of an obstacle.

Finally, we expect that the mathematical analysis used in this paper may be useful for the description of other beams or diffraction patterns that are theoretically infinite in extent, as Talbot self-images or computer-generated Fresnel holograms [36].

Appendix A. Asymptotic behavior of the functions $c_m(r',z)$

If we consider $N_F \gg 1$ then, we may write the diffraction of the pupil function as:

$$P(\mathbf{r}') \approx \exp(ikz)\mathrm{circ}\left(\frac{\mathbf{r}'}{R}\right), \qquad (A.1)$$

where $\mathrm{circ}(\mathbf{r}'/R)$ is a circle function: this function is zero outside a circle of radius R and unity inside the circle. With this approximation, we may easily calculate the contribution to the function $c_m(\mathbf{r}',\mathbf{z})$ coming from the fact that the ring of radius r_1 lies on a region outside the geometrical

projection of the aperture. Then we wish to calculate:

$$c_m(\mathbf{r}',z) = \frac{(-1)^m}{2\pi} \int_0^{2\pi} \mathrm{circ}\left(\frac{x'+r_1\cos\beta}{R}, \frac{y'+r_1\sin\beta}{R}\right)$$
$$\times \exp(-\mathrm{i}m\beta)\mathrm{d}\beta. \tag{A.2}$$

For the sake of simplicity, let us write $x' = r'$ and $y' = 0$ (this is equivalent to consider $(r', \theta = 0)$ in cylindrical coordinates) and we will assume $R \geqslant r_1$. Two intervals have to be considered:

(i) $r' < R - r_1$: then $c_0 = 1$ and $c_m = 0$ for $m \neq 0$. In this interval we expect a perfect reconstruction of the SNB.
(ii) For $R - r_1 < r' < R + r_1$ the ring will have a sector which lies inside the circle. This sector will start and end in the points where the circumference that defines the aperture coincides with the ring; this happens for two angles $-\beta_0$ and β_0 that may be obtained by solving the following equation:

$$(r' + r_1\cos\beta)^2 + \left(r_1^2\sin\beta\right)^2 = R^2. \tag{A.3}$$

Solving for $\cos(\beta)$, we obtain:

$$\cos(\pm\beta_0) = \frac{R^2 - r_1^2 - r'^2}{2r'r_1}. \tag{A.4}$$

Using Eqs. (32) and (33), we may rewrite Eq. (A.2) as $c_m(\mathbf{r}',z) = \exp(-\mathrm{i}m\theta)d_m(\mathbf{r}',z)$ and:

$$d_m(\mathbf{r}',z) = \frac{(-1)^m}{2\pi} \int_{\beta_0}^{2\pi-\beta_0} \exp(-\mathrm{i}m\beta)\mathrm{d}\beta. \tag{A.5}$$

Performing the integral we obtain:

$$d_0(\mathbf{r}',z) = 1 - \frac{\beta_0}{\pi} \quad d_m(\mathbf{r}',z) = (-1)^{m+1}\frac{\sin(m\beta_0)}{m\pi}. \tag{A.6}$$

Note that $\beta_0 = 0$ for $r' = R - r_1$, $\beta_0 = \pi/2$ for $r' = (R^2 - r_1^2)^{1/2}$ and $\beta_0 = \pi$ for $r' = R + r_1$. The maximum value of $d_0(\mathbf{r}',z)$ is 1 but the maximum value of the other $d_m(\mathbf{r}',z)$ is $1/m\pi$. The function $d_m(\mathbf{r}',z)$ will show $0.5*m$ oscillations in this interval. Inside the geometric projection of the pupil,

for $r' < (R^2 - r_1^2)^{1/2}$ we expect then that $d_m(\mathbf{r}',z)$ will show $0.25*m$ oscillations. This means, for instance, that for $r' = (R^2 - r_1^2)^{1/2}$ we expect $d_1(\mathbf{r}',z)$ to take its maximum value and $d_2(\mathbf{r}',z)$ to be near zero. Also, we may consider the functions $e_m(\mathbf{r}',z)$:

$$e_0(\mathbf{r}',z) = 1 - \frac{\beta_0}{\pi}$$
$$e_m(\mathbf{r}',z) = (-1)^{m+1}2\frac{\sin(m\beta_0)}{m\pi}. \tag{A.7}$$

Analogous comments apply to these functions.

References

[1] J. Durnin, J. Opt. Soc. Am. A 4 (1987) 651.
[2] J. Durnin, J.J. Miceli Jr., J.H. Eberly, Phys. Rev. Lett. 58 (1987) 1499.
[3] G. Indebetouw, J. Opt. Soc. Am. A 6 (1989) 150.
[4] J.C. Gutierrez-Vega, M.D. Iturbe-Castillo, S. Chávez-Cerda, Opt. Lett. 25 (2000) 1493.
[5] S. Chávez-Cerda, J.C. Gutiérrez-Vega, G.H.C. New, Opt. Lett. 26 (2001) 1803.
[6] M.A. Bandres, J.C. Gutiérrez-Vega, S. Chávez-Cerda, Opt. Lett. 29 (2004) 44.
[7] S. Ruschin, J. Opt. Soc. Am. A 11 (1994) 3224.
[8] S. Chávez-Cerda, G.S. McDonald, G.H.C. New, Opt. Commun. 123 (1996) 225.
[9] L. Vicari, Opt. Commun. 70 (1989) 263.
[10] Z. Bouchal, Opt. Lett. 27 (2002) 1376.
[11] J. Salo, J. Fagerholm, A.T. Friberg, M.M. Salomaa, Phys. Rev. E 62 (2000) 4261.
[12] R.M. Herman, T.A. Wiggins, J. Opt. Soc. Am. A 8 (1991) 932.
[13] J.H. McLeod, J. Opt. Soc. Am. 44 (1954) 592.
[14] R. Arimoto, C. Saloma, T. Tanaka, S. Kawata, Appl. Opt. 31 (1992) 6653.
[15] Z.L. Horvath, et al., J. Opt. Soc. Am. A 14 (1997) 3009.
[16] A. Vasara, J. Turunen, A.T. Friberg, J. Opt. Soc. Am. A 6 (1989) 1748.
[17] C. Paterson, R. Smith, Opt. Commun. 124 (1996) 121.
[18] J.A. Davis, E. Carcole, D.M. Cottrell, Appl. Opt. 35 (1996) 593.
[19] N. Chattrapiban, et al., Opt. Lett. 28 (2003) 2183.
[20] T. Aruga, Appl. Opt. 36 (1997) 3762.
[21] T. Aruga, et al., Appl. Opt. 38 (1999) 3152.
[22] J.C. Gutierrez-Vega, et al., Opt. Commun. 195 (2001) 35.
[23] S. Chavez-Cerda, et al., J. Opt. B 4 (2002) 52.
[24] J. Salo, M.M. Salomaa, Phys. Rev. E 67 (2003) 056609.
[25] Z. Bouchal, J. Wagner, M. Chlup, Opt. Commun. 151 (1998) 207.
[26] J.A. Davis, E. Carcole, D.M. Cottrell, Appl. Opt. 35 (1996) 599.
[27] K. Wang, L. Zeng, Ch. Yin, Opt. Commun. 216 (2003) 99.

[28] R.P. MacDonald, et al., Opt. Commun. 122 (1996) 169.
[29] J.A. Davis, E. Carcole, D.M. Cottrell, Appl. Opt. 35 (1996) 2159.
[30] V. Garcés-Chávez, et al., Nature 419 (2002) 145.
[31] M. Erdeyi, et al., J. Vac. Sci. Technol. B 15 (1997) 287.
[32] S. De Nicola, Opt. Commun. 80 (1991) 299.
[33] P.L. Overfelt, C.S. Kenney, J. Opt. Soc. Am. A 8 (1991) 732.
[34] A.T. Friberg, J. Opt. Soc. Am. A 13 (1996) 743.
[35] G.W. Forbes, J. Opt. Soc. Am. A 13 (1996) 1816.
[36] J.W. Goodman, Introduction to Fourier Optics, McGraw-Hill, New York, 1988 (Chapter 4).
[37] E. Carcole, J.A. Davis, D.M. Cottrell, Appl. Opt. 34 (1995) 5118.
[38] A.J. Cox, J. D'Anna, Opt. Lett. 17 (1992) 232.
[39] T. Cathey, Optical Information Processing and Holography, Wiley, New Cork, 1974 (Chapter 2).
[40] R. Liu, Bi-Zhen Dong, Guo-Zhen Yang, Ben-Yuan Gu, J. Opt. Soc. Am. A 15 (1998) 144.
[41] J.N. Provost, J.L. de Bougrenet de la Tocnaye, J. Opt. Soc. Am. A 14 (1997) 2748.
[42] M. Born, E. Wolf, Principles of Optics, Cambridge University Press, Cambridge, 2002 (Chapter 8).